Total Pressure Losses Minimization in Turbomachinery Cascades, using a New Continuous Adjoint Formulation

D.I. Papadimitriou, K.C. Giannakoglou

Laboratory of Thermal Turbomachines, National Technical University of Athens,
P.O. Box: 64069, Athens 157 10, Greece, e-mail: kgianna@central.ntua.gr

ABSTRACT

A new continuous adjoint formulation for the optimization of cascade airfoils with minimum total pressure losses, i.e. an objective function which has never been used before along with the continuous adjoint, is presented. To support a steepest descent algorithm, the adjoint method computes the gradient of the objective function with respect to the design variables. The function is defined as the difference in total pressure between the inlet to and the outlet from the cascade. In contrast to other known continuous adjoint approaches in aerodynamics (such as inverse designs based on target pressure distributions or drag–lift optimization for isolated airfoils), where the functional is defined over the parameterized solid walls, the present functional consists of integrals over the inlet/outlet boundaries only. To cope with this particular situation, the method of characteristics is used to impose inlet/outlet adjoint boundary conditions. It is worth noting that the objective function gradient is expressed as an integral over the solid walls. The minimization of losses in linear and peripheral compressor cascades, constrained by the desirable flow turning and minimum allowed blade thickness, are demonstrated.

INTRODUCTION

In optimization problems, an efficient means to compute the gradient of an objective function with respect to the design variables is the so–called adjoint approach. The exploitation of the relevant control theory concepts for the purpose of optimization is due to Pironneau (1984), for problems governed by elliptic pde's, whereas the adjoint method within the field of aeronautics was first proposed by Jameson (1988). Since then, the adjoint method has found widespread use in internal and external aerodynamics, Jameson et al. (1998), including turbomachinery applications, Campobasso et al. (2003), even for unsteady flows, Duta et al. (2002).

Recent and ongoing relevant research, Jameson and Kim (2003), Papadimitriou and Giannakoglou (2007), Nadarajah et al. (2006), mostly focuses on (a) the reduction of the computational cost of the optimization loop which includes the repetitive solution of the state and adjoint equations, (b) the development of continuous adjoint equations for new objective functions in the form of field and/or boundary integrals and (c) formulations which avoid the presence of field integrals in the final expression for the objective function gradient, and, thus, the need for repetitive remeshing of domains with bifurcated shapes to account for variations in grid–related quantities.

With respect to (a), incomplete gradient methods, Mohammadi and Pironneau (2004), which may skip the solution of adjoint equations have been proposed. Regarding (b), the need for handling objective functions related to "field" viscous terms for turbomachinery applications, in particular, is evident. The present authors have recently proposed an entropy generation based objective function and the corresponding continuous adjoint approach, Papadimitriou and Giannakoglou (2007). Note that this resulted to a gradient expression free of field integrals, although the objective function itself was a field integral. This is also related to point (c), where another noticeable contribution is the so–called reduced gradient approach which gives gradient expressions that include only boundary integrals and, thus, overcomes "artifices" for computing grid sensitivities, Jameson and Kim (2003).

In this paper, the continuous adjoint approach for an objective function which expresses the total pressure losses in turbomachinery cascades is presented. Although the objective function is nothing

more than the difference in averaged (integrated) total pressure between the inlet and outlet, this has never been used as objective function in the context of continuous adjoint. The need of setting up and solving design optimization problems in which the objective function is a line (in 2D) or a surface (in 3D) integral defined remotely from the parameterized solid walls can be found in other applications, such as the design of diffusers with minimum exit flow deviation, Iollo et al. (2001), the design of fans and propellers for maximum thrust, Ferlauto and Iollo (2001), or the design of wings at supersonic flow for sonic boom reduction, Nadarajah et al. (2006). However, none of them copes with total pressure losses minimization in cascades; furthermore, the present adjoint formulation accounts for the Navier-Stokes equations (with the Spalart–Allmaras turbulence model) and not for the Euler ones (as the three aforementioned papers do). The discrete adjoint formulation for the present functional, which is straightforward to develop, has been presented in Papadimitriou and Giannakoglou (2006).

FLOW EQUATIONS AND OBJECTIVE FUNCTION

To illustrate the derivation of the adjoint equations and boundary conditions, we first write the Favre–averaged viscous flow equations of compressible fluids in their usual vector form as

$$\frac{\partial \vec{U}}{\partial t} + \frac{\partial \vec{f}_i^{inv}}{\partial x_i} - \frac{\partial \vec{f}_i^{vis}}{\partial x_i} = \vec{0} \tag{1}$$

where

$$\vec{U} = \begin{bmatrix} \rho \\ \rho\vec{u} \\ E \end{bmatrix} , \vec{f}_i^{inv} = \begin{bmatrix} \rho u_i \\ \rho u_i \vec{u} + p\vec{\delta}_i \\ u_i(E+p) \end{bmatrix} , \vec{f}_i^{vis} = \begin{bmatrix} 0 \\ \vec{\tau}_i \\ u_j\tau_{ij} + q_i \end{bmatrix} \tag{2}$$

$\vec{\tau}_i$ is the vector of the viscous stresses, with

$$\tau_{ij} = \mu\left(\frac{\partial u_i}{\partial x_j} + \frac{\partial u_j}{\partial x_i}\right) + \lambda\,\delta_{ij}\frac{\partial u_k}{\partial x_k} \quad , \quad \lambda = -\frac{2}{3}\mu \tag{3}$$

and $\vec{\delta}_i$ are the Kronecker symbols, $\vec{u}$ is the velocity vector, $q_i = k\frac{\partial T}{\partial x_i}$ and $E = \rho e + \frac{1}{2}\rho u_i^2$. Eq. 1 along with the turbulence model equations and appropriate boundary conditions constitute the primal problem (or state) equations to be satisfied on flow domains defined by the initial, any intermediate (during the optimization loop) and the final–optimal blade or airfoil shape.

For the numerical solution of eq. 1, an in–house software is used. This is a time–marching code for structured and unstructured grids which uses a point–implicit, upwind, finite–volume discretization, with vertex–centered storage of flow variables. Inviscid fluxes at finite volume interfaces are computed using the upwind scheme of Roe (1981), with second–order variable extrapolation. For stretched grids, the limiter presented by van Albada et al. (1982), is used. The parallelized solver, enhanced with multigrid acceleration, is described at length by Lambropoulos et al. (2004). The one–equation turbulence model by Spalart and Allmaras (1994) is solved separately from the flow equations, at each pseudo–time step.

As already mentioned, the objective functional is defined as the difference between total pressure integrals over the inlet S_i to and outlet S_o from of the flow domain Ω, namely

$$F = \int_{S_i} p_t dS - \int_{S_o} p_t dS \tag{4}$$

with variation

$$\delta F = - \int_{S_o} \delta p_t dS \tag{5}$$

since inlet p_t remains invariant. Note that δF depends solely on p_t variations, and, consequently, on $\delta\vec{U}$ over the exit boundary. Variations in geometrical quantities do not appear in eq. 5. However, by formulating the augmented objective function F_{aug} and after some mathematical rearrangements, δF_{aug} is expressed in terms of variations in geometrical quantities directly linked to variations in the design variables that control the shape.

THE ADJOINT PROBLEM

The continuous adjoint formulation may be derived without considering the type of grid (structured or unstructured) used, by relying upon the identity

$$\delta\left(\frac{\partial\Phi}{\partial x_i}\right)=\frac{\partial(\delta\Phi)}{\partial x_i}-\frac{\partial\Phi}{\partial x_k}\frac{\partial(\delta x_k)}{\partial x_i} \tag{6}$$

which holds for any scalar Φ, Papadimitriou and Giannakoglou (2007). The variation in F_{aug} is formed by adding δF (eq. 5) to the variation in the flow equations multiplied by the adjoint variables $\vec{\Psi}$, as follows

$$\delta F_{aug}=\delta F+\int_\Omega \vec{\Psi}^T\delta\left(\frac{\partial\vec{f}_i^{inv}}{\partial x_i}-\frac{\partial\vec{f}_i^{vis}}{\partial x_i}\right)d\Omega \tag{7}$$

Using eq. 6, the integral of the variation in inviscid or viscous terms may be written as

$$\int_\Omega \vec{\Psi}^T\delta\left(\frac{\partial\vec{f}_i}{\partial x_i}\right)d\Omega=\int_\Omega \vec{\Psi}^T\frac{\partial(\delta\vec{f}_i)}{\partial x_i}d\Omega-\int_\Omega \vec{\Psi}^T\frac{\partial\vec{f}_i}{\partial x_k}\frac{\partial(\delta x_k)}{\partial x_i}d\Omega \tag{8}$$

We first consider the inviscid term; integration by parts and the Gauss' divergence theorem yields

$$\begin{aligned}\int_\Omega \vec{\Psi}^T\frac{\partial(\delta\vec{f}_i^{inv})}{\partial x_i}d\Omega &= -\int_\Omega \delta\vec{U}^T\left(A_i^T\frac{\partial\vec{\Psi}}{\partial x_i}\right)d\Omega+\int_{S_{i,o}}\delta\vec{U}^T(A_n^T\vec{\Psi})dS\\ &+ \int_{S_w}\Psi_{i+1}n_i\delta p dS+\int_{S_w}(\Psi_{i+1}p-\vec{\Psi}^T\vec{f}_i^{inv})\delta(n_i dS)\end{aligned} \tag{9}$$

where S_w stands for the impermeable ($u_i n_i=0$) solid walls, $\vec{n}$ is the outwards unit normal vector, A_i is the Jacobian matrix and $A_n=A_i n_i$.

The second term on the r.h.s. of eq. 8, after an additional integration by parts, becomes

$$\begin{aligned}-\int_\Omega \vec{\Psi}^T\frac{\partial\vec{f}_i^{inv}}{\partial x_k}\frac{\partial(\delta x_k)}{\partial x_i}d\Omega &= \int_\Omega \frac{\partial\vec{U}}{\partial x_k}^T(A_i{}^T\frac{\partial\vec{\Psi}}{\partial x_i})\delta x_k d\Omega+\int_\Omega \vec{\Psi}^T\frac{\partial}{\partial x_k}(\frac{\partial\vec{f}_i^{inv}}{\partial x_i})\delta x_k d\Omega\\ &- \int_S \vec{\Psi}^T\frac{\partial\vec{f}_i^{inv}}{\partial x_k}\delta x_k n_i dS\end{aligned} \tag{10}$$

Regarding the viscous term in eq. 7, the first term on the r.h.s. of eq. 8 (for $\vec{f}_i^{vis}$), after being twice integrated by parts, becomes

$$\begin{aligned}-\int_\Omega \vec{\Psi}^T\frac{\partial(\delta\vec{f}_i^{vis})}{\partial x_i}d\Omega &= \int_\Omega\left[\delta\tau_{ij}\left(\frac{\partial\Psi_{j+1}}{\partial x_i}+u_j\frac{\partial\Psi_m}{\partial x_i}\right)+\delta u_j\left(\tau_{ij}\frac{\partial\Psi_m}{\partial x_i}\right)+\delta q_i\frac{\partial\Psi_m}{\partial x_i}\right]d\Omega\\ &- \int_S[(\Psi_{i+1}+u_i\Psi_m)\delta\tau_{ij}+\Psi_m\tau_{ij}\delta u_i+\Psi_m\delta q_j]n_j dS\end{aligned} \tag{11}$$

where $m=4$ (2D) or $m=5$ (3D). Further analysis of $\delta\tau_{ij}$ or δq_i terms is beyond the scope of this paper and the interested reader should refer to Papadimitriou and Giannakoglou (2007). We also omit

the development of the boundary integral in eq. 11 which, for solid walls (S_w), should be based on the identity $\tau_{ij}n_in_j=0$, Papadimitriou and Giannakoglou (2007). The second integral on the r.h.s. of eq. 7 can be developed similarly to its inviscid counterpart and the reader may readily work it out by himself.

If the previous expressions are substituted into eq. 6, a lengthy expression for δF_{aug} is obtained. Field terms depending on $\delta\vec{U}$ are eliminated by satisfying the field adjoint equations, namely

$$\frac{\partial\vec{\Psi}}{\partial t}-A_i^T\frac{\partial\vec{\Psi}}{\partial x_i}-M^{-T}\vec{K}=\vec{0} \tag{12}$$

where $M=\partial\vec{U}/\partial\vec{W}$, $\vec{W}=[\rho,\vec{u},p]$ is the vector of primitive flow variables and $\vec{K}=(K_1,...,K_m)^T$ is defined as follows

$$K_1=-\frac{T}{\rho}\frac{\partial}{\partial x_i}\left(k\frac{\partial\Psi_m}{\partial x_i}\right)\ ,\ K_{i+1}=\frac{\partial G_{ij}}{\partial x_j}-\tau_{ij}\frac{\partial\Psi_m}{\partial x_j}\ ,\ i\in[1,m-1]\ ,\ K_m=\frac{T}{p}\frac{\partial}{\partial x_i}\left(k\frac{\partial\Psi_m}{\partial x_i}\right) \tag{13}$$

with $G_{ij}=\mu\left(\frac{\partial\Psi_{j+1}}{\partial x_i}+u_j\frac{\partial\Psi_m}{\partial x_i}+\frac{\partial\Psi_{i+1}}{\partial x_j}+u_i\frac{\partial\Psi_m}{\partial x_j}\right)+\lambda\,\delta_{ij}\left(\frac{\partial\Psi_{k+1}}{\partial x_k}+u_k\frac{\partial\Psi_m}{\partial x_k}\right)$.

Boundary conditions for $\Psi_i, 1<i<m$, over S_w are derived so as to eliminate the boundary integrals which include $\delta\vec{U}$ or $\delta\vec{W}$ other than δu_i since the latter automatically cancel. Hence, by eliminating terms such as $\int_{S_w}\Psi_{i+1}n_i\delta p dS$, $\int_{S_w}\frac{\Psi_{i+1}}{n_i}[\delta\tau_{ij}n_in_j+\tau_{ij}\delta(n_in_j)]dS$, etc, homogeneous Dirichlet conditions for $\Psi_i, 1<i<m-1$, are obtained. On the other hand, the solid wall condition on Ψ_m depends on the local condition on temperature: $\Psi_m=0$ for given wall temperature and $\frac{\partial\Psi_m}{\partial n}=0$ for adiabatic walls.

Conditions on $\vec{\Psi}$ over S_i and S_o are obtained from the elimination of the inlet/outlet boundary integrals. Integrals depending on spatial derivatives of flow variables are, there, neglected. The second integral on the r.h.s. of eq. 9 is analyzed as

$$\int_{S_{i,o}}\delta\vec{U}^TA_n^T\vec{\Psi}dS=\int_{S_{i,o}}\vec{\Psi}^TA_n\delta\vec{U}dS=\int_{S_{i,o}}\vec{\Psi}^TP\Lambda P^{-1}\delta\vec{U}dS=\int_{S_{i,o}}\left[(P\Lambda)^T\vec{\Psi}\right]^T\delta\vec{V}dS \tag{14}$$

where P and P^{-1} are formed by the right and left eigenvectors of A_n, respectively, and Λ is the diagonal matrix with the eigenvalues of A_n. $\vec{V}$ is the vector of characteristic flow variables with $\delta\vec{V}=P^{-1}\delta\vec{U}$.

With similar considerations, eq. 5 may be written as

$$-\int_{S_o}\delta p_t dS=-\int_{S_o}\frac{\partial p_t}{\partial\vec{W}}^TL\delta\vec{V}dS \tag{15}$$

where L is the matrix with the right eigenvectors of the Jacobian matrix of $\vec{W}$. In 2D problems, for instance

$$\frac{\partial p_t}{\partial\vec{W}}=g\left[\frac{u_i^2}{2}\ ,\ \rho u_1\ ,\ \rho u_2\ ,\ \left(1-\frac{u_i^2}{2\gamma}\frac{\rho}{p}\right)\right] \tag{16}$$

where $g=\left(1+\frac{u_i^2}{2\gamma}\frac{(\gamma-1)p}{\rho}\right)$. Along S_o, the sum of the corresponding terms in eqs. 14 and 15 gives $\int_{S_o}\left\{\left[(P\Lambda)^T\vec{\Psi}\right]^T-\frac{\partial p_t}{\partial\vec{W}}^TL\right\}\delta\vec{V}dS$ and the terms in brackets determine the exit conditions on $\vec{\Psi}$, in conformity to the boundary conditions for the flow variables. The physical interpretation is simple. Characteristic flow variables traveling from outside Ω remain constant, so their variation is zero. The

corresponding adjoint variables are extrapolated from the interior of the flow domain. The $\vec{\Psi}$ variables related to $\delta\vec{V}$ traveling from the interior of Ω are computed by solving

$$\left[(P\Lambda)^T\vec{\Psi}\right]^T + \frac{\partial p_t}{\partial \vec{W}}^T L = 0 \tag{17}$$

Along S_i, $(P\Lambda)^T\vec{\Psi}$ should be zeroed, as in inviscid flows. After eliminating field and boundary integrals depending on $\delta\vec{U}$ or $\delta\vec{W}$, integrals which include variations in geometrical quantities along the solid wall read

$$\begin{aligned}\delta F_{aug} &= \int_{S_w}(\Psi_i p - \vec{\Psi}^T\vec{f}_i^{inv})\delta(n_i dS) - \int_{S_w}\vec{\Psi}^T\left(\frac{\partial\vec{f}_i^{inv}}{\partial x_k} - \frac{\partial\vec{f}_i^{vis}}{\partial x_k}\right)\delta x_k n_i dS \\ &+ \int_{S_w}\frac{\Psi_{i+1}}{n_i}\tau_{ij}\delta(n_i n_j)dS + \int_{S_w}\Psi_m q_j\delta(n_j dS) - \int_{S_w}\frac{\partial u_i}{\partial x_l}G_{ij}\delta x_l n_j dS\end{aligned} \tag{18}$$

Eq. 18 produces the sensitivity derivatives, which are necessary for the descent optimization algorithm. As prerequisite, the shape parameterization should be defined and expressions for δn_i, $\delta(dS)$, δx_i should be devised. The absence of field integrals in eq. 18 should be noted.

OPTIMIZATION OF TURBOMACHINERY CASCADES

The adjoint method is applied to the loss minimization of 2D and 3D turbomachinery cascades. The blade contours/surfaces are parameterized using Bézier polynomials. Each blade side is parameterized separately. The cascade pitch and stagger angles are considered to be known. Geometrical constraints to account for very thin blades or airfoils are imposed. Thicknesses are computed at several chordwise and spanwise (in 3D) locations and are not allowed to decrease below a fraction of their initial values. The inequality constraints are handled using the augmented Lagrange multiplier method, by simultaneously decreasing the steepest descent stepsize.

2D Compressor and Turbine Cascade Designs

The first two applications are concerned with the optimization of a compressor and a turbine cascade airfoil, for minimum p_t losses at given flow conditions. For the compressor cascade: $M_{out,is} = 0.45$, $\alpha_{in} = 47^o$, $Re = 8\times10^5$ whereas for the turbine: $M_{out,is} = 0.75$, $\alpha_{in} = 0^o$, $Re = 10^6$.

The blade airfoils are parameterized using 13 and 15 control points for the compressor and the turbine, respectively. Their chordwise coordinates are kept constant and only the normal ones are allowed to vary. Each airfoil is parameterized at zero stagger angle and, then, rotated to the known stagger angle. The pitch is equal to $0.7C$ for the compressor and $0.8C$ for the turbine cascade (C:chord length).

Fig. 1 illustrates the reduction in p_t losses during the optimization process, in both cascade problems. The horizontal axis counts cycles; each cycle corresponds to the numerical solution of the state (mean flow and turbulence model) equations followed by that of the adjoint equations, the computation of sensitivity derivatives according to eq. 18, the treatment of constraints and, finally, a steepest descent algorithm with constant stepsize. The vertical axis stands for the non–dimensional total pressure loss coefficient, defined as $\omega = \frac{\overline{p}_{t,in} - \overline{p}_{t,out}}{\overline{p}_{t,in} - \overline{p}_{in}}$ for the compressor and $\omega = \frac{\overline{p}_{t,in} - \overline{p}_{t,out}}{\overline{p}_{t,out} - \overline{p}_{out}}$ for the turbine; overline denotes pitchwise averaging. The initial shapes are existing airfoils used to set the thickness constraints. With respect to the latter, fig. 2 shows the degree of constraint violation at each cycle. Note that, a zero value means that no constraint is violated.

The gradient values for the initial and optimal airfoils are illustrated in fig. 3. Positive gradient values correspond to the suction side control points and the negative, or low–valued positive ones to

the pressure side. These distributions reveal the thickness reduction tendency for the compressor and turbine blades.

It is important to pay more attention to the flow related constraint (desired flow turning) rather than the geometric constraint (minimum thickness). For this purpose, the compressor case was analyzed twice: with and without taking into account the flow turning constraint. Results are shown together in fig. 4. As expected, the optimization method had the tendency to further reduce the p_t losses by modifying the flow turning. Hence, it is due to the flow turning constraint that the optimal airfoil gives $\omega = 0.027$ instead of $\omega = 0.022$ which was obtained for flow turning, different than the desired one.

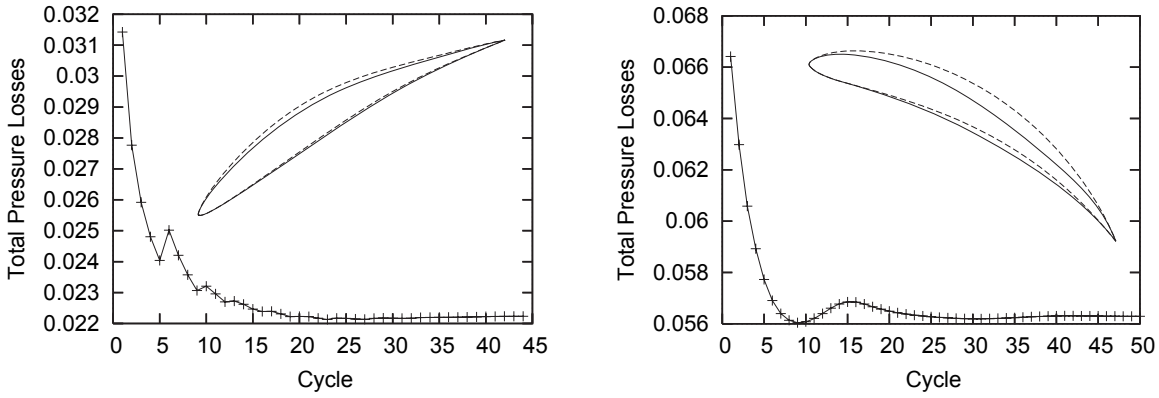

Figure 1: 2D compressor and turbine cascade optimization. Reduction in total pressure loss coefficient. The initial (dashed line) and optimal (continuous line) airfoil shapes are also shown.

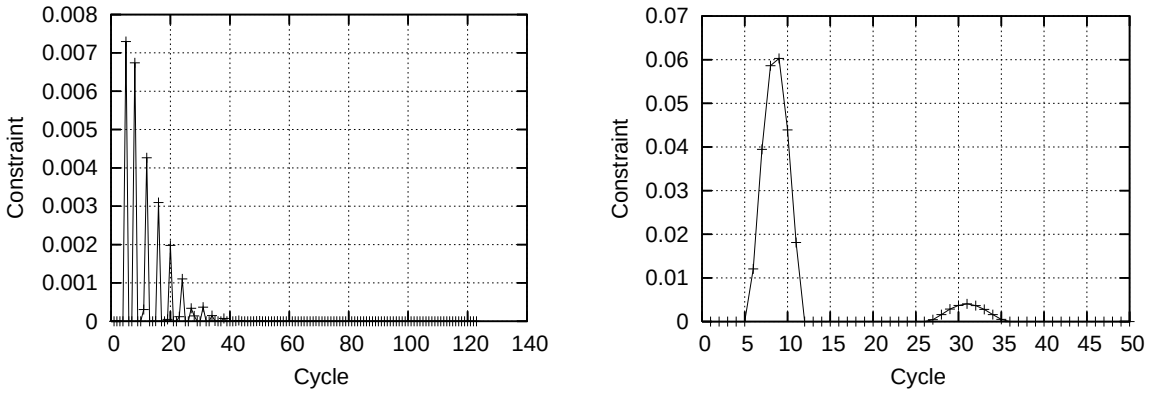

Figure 2: 2D compressor and turbine cascade optimization. Degree of constraints' violation during the optimization cycles. Zero constraint values correspond to feasible solutions.

3D Compressor Design

In this study, a 3D peripheral compressor stator is optimized for minimum p_t losses. The shape of the blade has been optimized in a previous paper by the authors, Papadimitriou and Giannakoglou (2007), by considering minimum entropy generation due to cascade profile losses. This case is revisited here, the target now being the minimization of p_t losses.

The flow conditions are $M_{out,is} = 0.4$, $\alpha_{in,per} = 0$, $\alpha_{in,rad} = 0$ and $Re = 10^5$. An H-type structured grid with $191 \times 55 \times 71$ nodes is used. The blade is parameterized using 5 control points in the spanwise and 13 in the chordwise direction. The blade hub and shroud control points are free to vary and the remaining control points are obtained by linear interpolation. Constraints on minimum blade thickness are also imposed here, computed at various positions along the spanwise and chordwise directions. The pressure distribution over the optimal blade is shown in fig. 5.

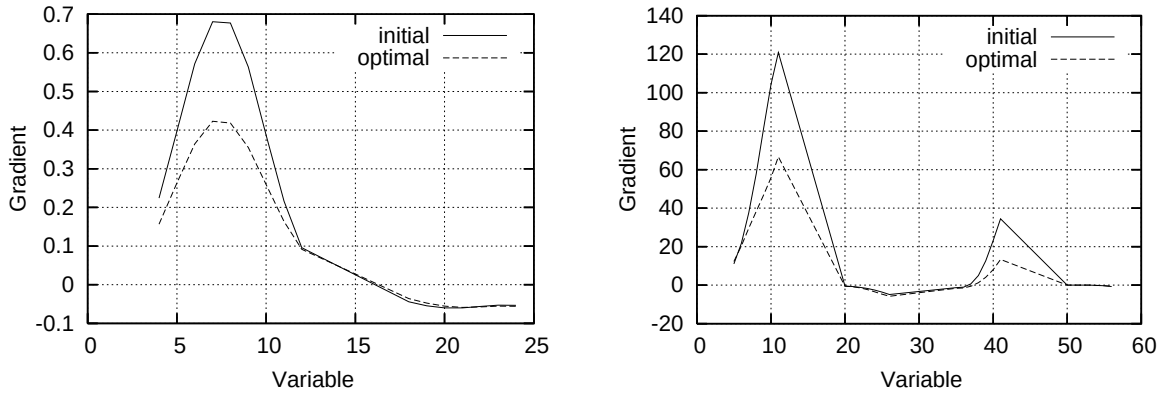

Figure 3: 2D compressor and turbine cascade optimization. Functional gradient values for the initial and optimal set of control points. The first half variables correspond to the normal–to–chord coordinates of the suction side control points and the remaining correspond to those parameterizing the pressure side. At the optimal solution, the objective function gradient is far from being zeroed due to the imposed costraints. Note that the vertical axis represents non–penalized (due to the constraints) total pressure losses.

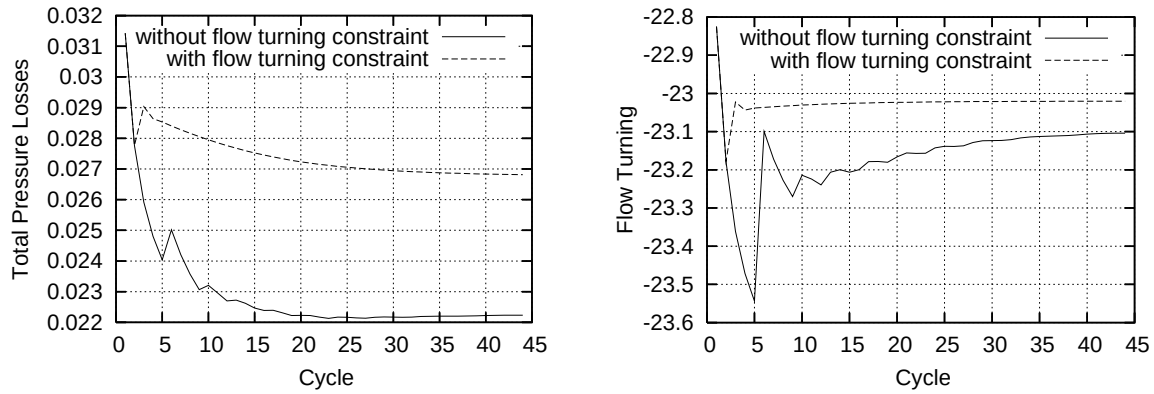

Figure 4: 2D compressor and turbine cascade optimization. Reduction in total pressure loss coefficient, left, and in flow turning angle, right, with and without taking into account the "equality" constraint on flow turning.

The total pressure losses reduction and the constraint violation measures are shown in fig. 6, which demonstrates the same thinning tendency as in the previous 2D cases. The initial and optimal control points at hub and tip are shown in fig. 7, while the corresponding contours are illustrated in fig. 8. In the same figures, we repeat the optimal shapes computed by Papadimitriou and Giannakoglou (2007), for the same case and minimum entropy generation. A similar tendency is observed and small differences are due to the slightly different initial set of free design variables.

CONCLUSIONS

This paper develops, demonstrates and assesses a continuous adjoint approach for the shape optimization of turbomachinery cascades so as to minimize total pressure losses. Despite the form of the objective function which includes integrals over the inlet to and the outlet from the cascade, the expression of the objective function gradient with respect to the design variables contains only integrals along the solid walls, which is advantageous since it avoids unnecessary remeshings and, thus, reduces the total CPU cost. Demonstrations on compressor and turbine, 2D and 3D cascade

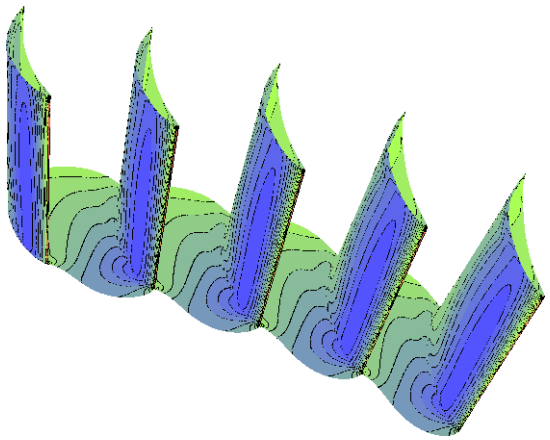

Figure 5: 3D compressor blade optimization. Pressure distribution over the optimal blade. Minimum pressure: 1.86, maximum pressure: 2.55, increment: 0.0345.

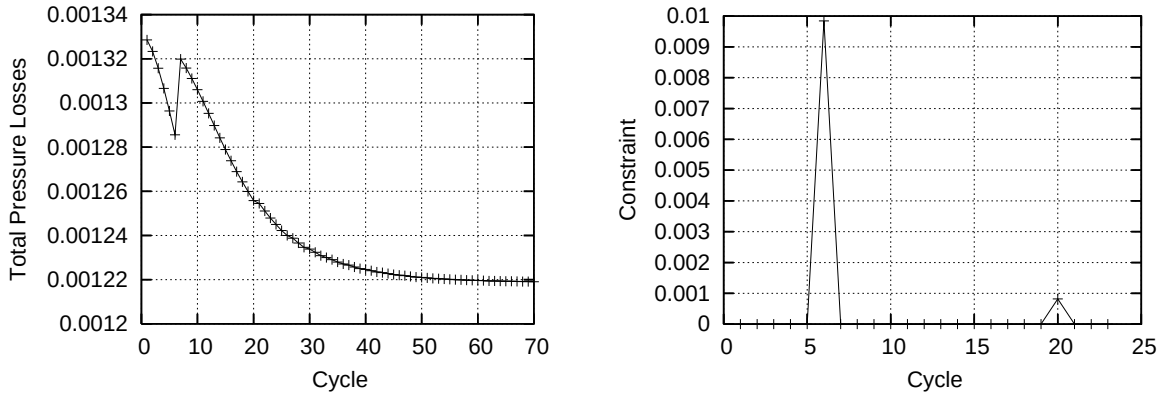

Figure 6: 3D compressor blade optimization. Convergence of the total pressure losses functional, left and sum of violated constraints, right.

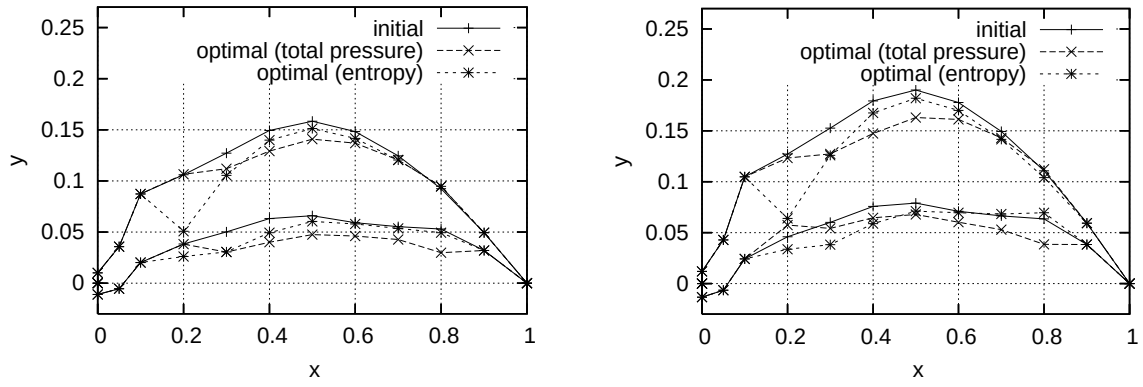

Figure 7: 3D compressor blade optimization. Initial and optimal sets of control points for the blade hub and tip using the total pressure loss functional proposed in the present paper and the entropy generation functional, presented in Papadimitriou and Giannakoglou (2007).

designs, indicate that the method performs satisfactorily. Flow and geometric constraints are taken into consideration.

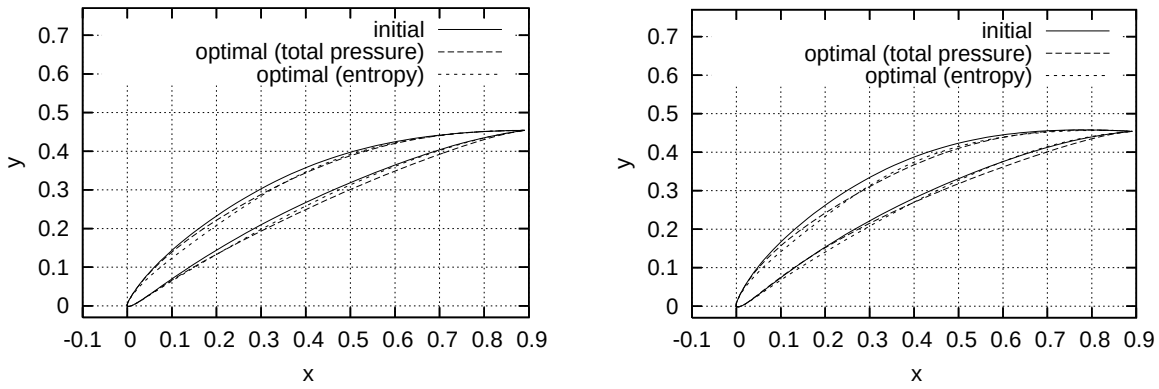

Figure 8: 3D compressor blade optimization. Initial and optimal contours for the blade hub and tip using the total pressure loss functional proposed in the present paper and the entropy generation functional, presented in Papadimitriou and Giannakoglou (2007).

ACKNOWLEDGEMENT

The first author was supported by a grant from the Beneficial Foundation Alexandros S. Onasis.

REFERENCES

M.S. Campobasso, M.C. Duta, and M.B. Giles. Adjoint calculation of sensitivities of turbomachinery objective functions. *AIAA Journal of Propulsion and Power*, 19(4), 2003.

M.C. Duta, M.B. Giles, and M.S. Campobasso. The harmonic adjoint approach to unsteady turbomachinery design. *International Journal for Numerical Methods in Fluids*, 40(3-4):323–332, 2002.

M. Ferlauto and A. Iollo. Fan and propeller design via inverse problem adjoint equations. ISABE-2001-1160, 2001.

A. Iollo, M. Ferlauto, and L. Zannetti. An aerodynamic optimization method based on the inverse problem adjoint equations. *Journal of Computational Physics*, 173:87–115, 2001.

A. Jameson. Aerodynamic design via control theory. *Journal of Scientific Computing*, 3:233–260, 1988.

A. Jameson and S. Kim. Reduction of the adjoint gradient formula in the continous limit. AIAA-2003-0040, AIAA 41th Aerospace Sciences Meeting and Exhibit, Reno NV, January 2003, 2003.

A. Jameson, N. Pierce, and L. Martinelli. Optimum aerodynamic design using the Navier-Stokes equations. *Journal of Theoretical and Computational Fluid Dynamics*, 10:213–237, 1998.

N.K. Lambropoulos, D.G. Koubogiannis, and K.C. Giannakoglou. Acceleration of a Navier-Stokes equation solver for unstructured grids using agglomeration multigrid and parallel processing. *Journal of Computer Methods in Applied Mechanics and Engineering*, 193:781–803, 2004.

B. Mohammadi and O. Pironneau. Shape optimization in fluid mechanics. Annual Review of Fluid Mechanics, 2004, 2004.

S. Nadarajah, A. Jameson, and J. Alonso. An adjoint method for the calculation of remote sesnitivities in supersonic flow. *International Journal of Computational Fluid Dynamics*, 20(2):61–74, 2006.

D.I. Papadimitriou and K.C. Giannakoglou. A continuous adjoint method with objective function derivatives based on boundary integrals for inviscid and viscous flows. *Journal of Computers and Fluids*, 36:325–341, 2007.

D.I. Papadimitriou and K.C. Giannakoglou. A continuous adjoint method for the minimization of losses in cascade viscous flows. AIAA Paper 2006-0049, 2006.

O. Pironneau. *Optimal shape design for elliptic systems*. Springer-Verlag, New York, 1984.

P. Roe. Approximate Riemann solvers, parameter vectors, and difference schemes. *Journal of Computational Physics*, 43:357–371, 1981.

P.R. Spalart and S.R. Allmaras. A one-equation turbulence model for aerodynamic flows. *La Recherche Aerospatiale*, (1):5–21, 1994.

G.D. van Albada, B. van Leer, and W.W. Roberts. A comparative study of computational methods in cosmic gas dynamics. *Astronomy and Astrophysics*, 108:76–84, 1982.